

# A Novel Pneumatically Driven SU-8 Microvalve for High Speed Gas Chromatographic Applications

A. Nubile<sup>\*a</sup>, A. Poggi<sup>\*</sup>, E. Cozzani<sup>\*</sup>, I. Elmi<sup>\*</sup>, S. Zampolli<sup>\*</sup>, M. Messina<sup>\*</sup>, G.C. Cardinali<sup>\*</sup>, F. Mancarella<sup>\*</sup> and M. Belluce<sup>\*</sup>

<sup>\*</sup> CNR IMM, Via. P. Gobetti 101, 40129, Bologna, Italy, messina@bo.imm.cnr.it

<sup>a</sup> MIST E-R, Via. P. Gobetti 101, 40129, Bologna, Italy, nubile@bo.imm.cnr.it

## ABSTRACT

For the successful miniaturization of integrated fluidic devices, it is desirable to have a reliable non-leaking microvalve that can be used in various environments, in a wide temperature range and that is chemically inert. This work describes the design, fabrication and characterization of an innovative pneumatically driven microvalve based on an SU-8 actuating membrane, to be employed in high-speed gas chromatographic (HSGC) applications. In this scenario, a critical constrain is the volume of the microvalve, which needs to be as small as possible to reduce the response time of the chromatograph. The experimental characterization of the fabricated SU-8 microvalves indicates very good sealing properties and low actuating pressures, under different working conditions and in spite of the reduced volume.

**Keywords:** integrated fluidic microvalves, SU-8, high speed gas chromatography, microelectromechanical systems

## 1 INTRODUCTION

Microvalves are basic components of microfluidic systems, since they permit fluid transfer, switching and control. MEMS technology has provided an opportunity for microvalves to be packaged onto a board with integrated fluidic channels to interconnect all the parts [1]. For the successful miniaturization of integrated microfluidic devices involving MEMS technology, it is desirable to have a reliable non-leaking microvalve that can be used in various environments, in a wide temperature range and that is chemically inert [2].

In particular, this work describes the design, fabrication and characterization of an innovative pneumatically driven microvalve, based on an SU-8 actuating membrane, for HSGC applications. A second design constraint for these applications is the low actuating pressure required to close the microvalve: normally, for portable devices, the maximum pressure available to control the fluidic microvalves is limited by the tank which also furnishes the carrier gas.

This work is structured as follows: section 2 describes the design of the proposed microvalve, section 3 illustrates the fabrication process, section 4 describes the experimental

characterization and section 5 discusses the results obtained.

## 2 DESIGN

The produced microvalve consists of an SU-8 membrane layer deposited between two micromachined silicon wafers. On the upper wafer, the actuation hole extending all through the Si substrate is fabricated for enabling the deformation of the membrane. In the lower wafer, the fluidic circuit is manufactured. A schematic view describing the operation of the microvalve is shown in Fig.1: the microvalve, deflected by the actuating pressure, contacts the ring blocking the carrier gas path. The carrier gas volume flow rates are typically of the order of 1 – 5 sccm.

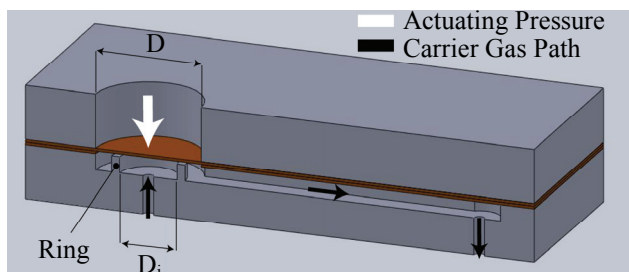


Figure 1: Microvalve main geometrical parameters and fluidic paths.

The fluid path inside the wafers consist of three parts: a rectangular channel having a length of 8200  $\mu\text{m}$ , a width  $W_{\text{ch}}$  of 240  $\mu\text{m}$  and a thickness of 30  $\mu\text{m}$ ; an inlet and outlet pipes with circular sections of 80  $\mu\text{m}$  diameter. All the microvalves studied in this work have a membrane thickness  $t$  of 10  $\mu\text{m}$  and a constant ring radial width of 20  $\mu\text{m}$ . The other main geometric parameters of the membranes are reported in Table 1, where  $D$  is the membrane diameter and  $D_i$  the supporting ring inner diameter.

The purpose of the ring is twofold: a) its height determine the microvalve discharge area  $A_v$

$$A_v = \pi D_i h \quad (1)$$

which allows to control the maximum flow rate and where  $h$  is the thickness of the second layer of SU-8 with a constant value for all microvalves of  $10\ \mu\text{m}$ , and  $b$ ) its radius  $D_i$  allows to change the actuating pressure: by increasing the value  $D_i$  up to the membrane diameter  $D$ , a higher actuating pressure is required to seal the carrier gas orifice.

This type of microvalve has also been designed for liquids as well, where the only design modification has consisted in a different fluidic channel width  $W_{\text{ch}}$ , ranging from  $30$  to  $120\ \mu\text{m}$ . For liquid applications, the volume flow rates are in the  $0.5 - 5\ \mu\text{l/s}$  range, depending on channels section and inlet liquid pressure, which for the applications of our interest varies between  $0.5$  bar to  $3$  bar. One advantage of our microvalve is that the realization process for liquid applications is the same as the one for gas-type devices.

Micro Valve	D ( $\mu\text{m}$ )	$D_i$ ( $\mu\text{m}$ )	$A_v$ ( $\text{mm}^2$ )
V1	800	180	0.00057
V2	800	200	0.00063
V3	800	520	0.00163
V4	500	150	0.00047
V5	500	200	0.00063
V6	500	320	0.00101

Table 1: microvalves main geometric parameters.

### 3 FABRICATION PROCESS

The microvalve was constructed by assembling and bonding two different sub-systems, which are separately fabricated: i) the upper part which consists of the SU8 membrane and the hole for the microvalve actuation on a silicon wafer (the actuation system); ii) the lower part which consists of a second silicon wafer with the flow channels and the microvalve ring (the microfluidic system).

The critical steps of the fabrication process are shown in Fig. 2. The fabrication starts with the processing of the microfluidic system. The front side of a  $300\ \mu\text{m}$  thick Si wafer is patterned and anisotropically etch for  $30\ \mu\text{m}$  using DRIE to create the microvalve ring and the carrier gas channel (Fig. 2a). From backside, DRIE etch process is carried out producing two holes to connect the carrier gas channel with the input and the output of the microfluidic gas system (Fig. 2b).

The manufacturing of the actuation system requires the patterning of a dioxide layer to define the actuation hole on the bottom side of another  $300\ \mu\text{m}$  thick Si wafer. On the top side, a first SU-8 layer  $10\ \mu\text{m}$  in thickness is deposited by spin coating, exposed to UV light and thermally treated to obtain the membrane layer of the microvalve. Then, a second SU-8 layer  $10\ \mu\text{m}$  in thickness is spun and exposed to UV light using the mask with the layout of the spacer. After the standard thermal process, the uncrosslinked SU-8 is developed and the pattern of the SU-8 spacer

between the membrane layer and the front side of the microfluidic system (Fig. 2c) is obtained.

Once the two sub-systems are fabricated a bonding protocol is applied, where the wafer sandwich is heated at  $110^\circ\text{C}$  at a pressure of  $4500\ \text{mbar}$  exploiting the SU-8 spacer as bonding layer (Fig. 2d).

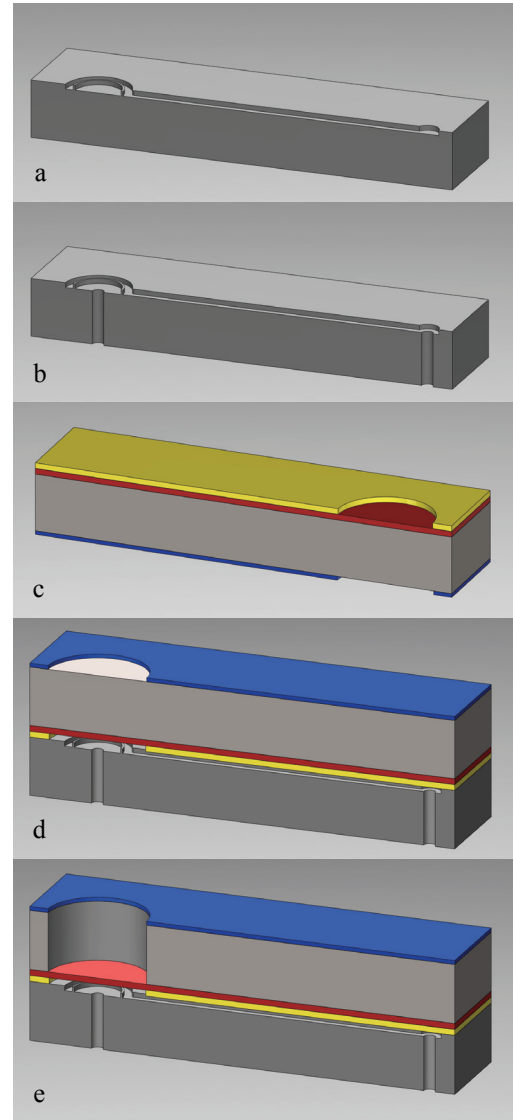


Figure 2: Process for the fabrication of the microvalve with SU-8 membrane.

The last step in the fabrication of the microvalve with SU-8 membrane is the Si etch to obtain the actuation hole. Using the previously patterned dioxide mask layer, a through-wafer DRIE process is employed to remove  $300\ \mu\text{m}$  of silicon releasing the SU-8 membrane (Fig. 2e). In Fig. 3, a micrograph of the resulting microvalve can be seen.

It should be stressed that all the fabrication process is performed at wafer level using standard MEMS technology.

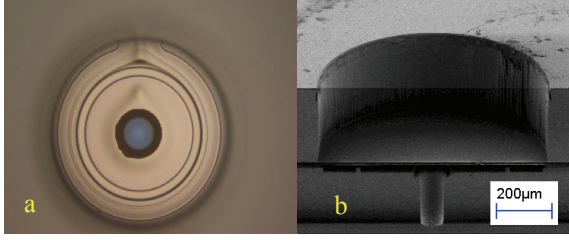


Figure 3: Micrograph of the microvalve V5 with SU-8 membrane: a) optical plan and b) SEM cross-section image.

## 4 CHARACTERIZATION

All the microvalves have been tested on a dedicated experimental setup, illustrated in Fig. 4. The experiments have been performed to determine the actuating pressure  $P_a$  required for sealing the microvalve, when the membrane is subjected to different carrier gas pressures  $P_{in}$  and to assess the durability of the microvalves under heavy duty cycles. To measure  $P_a$  the following procedure has been set up: a given pressure  $P_{in}$  has been set using Nitrogen as the working fluid and then the actuating pressure  $P_a$  has been slowly increased until the carrier gas flow stopped. The overpressure  $\Delta P$  has been then evaluated as:

$$\Delta P = P_a - P_{in} \quad (2)$$

The carrier gas pressure  $P_{in}$  varies between 1.6, 2.0 and 2.5 bar in all the experiments. These values represent the typical carrier gas pressure that the microvalve has to counterbalance for closing the orifice. Table 2 shows the averaged values obtained during the measurements campaign. Considering microvalves with the same diameter  $D$ , it can be observed the marked decrease in actuating pressure required for sealing with the lower ring diameters.

This result can be compared to the analytical expression for an elastic deflection of a clamped circular membrane under constant load [3]:

$$w(r) = \frac{3\Delta P(1-\nu)}{512Gt^3} [D^2 - (2r)^2]^2 \quad (3)$$

where  $G$  is the shear modulus and  $\nu$  the Poisson's ratio.

$P_{in}$ (bar)	$\Delta P$ (bar) $\pm$ 3% $\Delta P$					
	V1	V2	V3	V4	V5	V6
1.6	0.31	0.38	1.32	0.70	1.30	4.2
2.0	0.28	0.35	1.24	0.62	1.03	-
2.5	0.27	0.32	1.32	0.56	1.03	-

Table 2: Averaged measured microvalves actuating pressures.

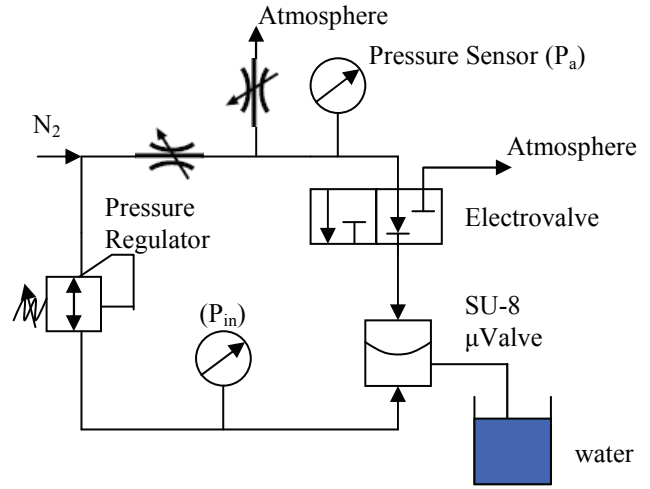


Figure 4: Schematic of the experimental setup.

The value of  $G = 1.23 \text{ GPa}$  has been experimentally determined using the technique described in [4]: the center displacement of a membrane, inserted in a valve without the ring, has been measured for different applied pressures. The resulting points have been then fitted using an appropriate polynomial: the determination of the polynomial's coefficients allows the computation of the Young's modulus. The Poisson's ratio has been assumed to be 0.22 as reported in [5]. The shear modulus is then computed as:

$$G = \frac{E}{2(1+\nu)} \quad (4)$$

Assuming that membranes with same diameters  $D$  and different ring diameter  $D_i$  seal the orifice when the membrane contacts the ring at the inner diameter, it is possible to evaluate the ratio between the actuating overpressure required as:

$$\frac{w_{Va}}{w_{Vb}} = \frac{\Delta P_{Va} (D^2 - D_{iVa}^2)^2}{\Delta P_{Vb} (b^2 - D_{iVb}^2)^2} \Rightarrow \frac{\Delta P_{Va}}{\Delta P_{Vb}} = \left( \frac{D^2 - D_{iVa}^2}{D^2 - D_{iVb}^2} \right)^2 \quad (5)$$

where the assumption  $w_{Va}/w_{Vb} = 1$  has been used. Using as reference the microvalves with lower  $D_i$ , it is possible to obtain an estimated  $\Delta P_{V3}/\Delta P_{V1} \sim 2.70$  for the microvalves with  $D = 800 \mu\text{m}$ , and  $\Delta P_{V5}/\Delta P_{V4} \sim 1.17$  for the microvalves with  $D = 500 \mu\text{m}$ . These values are lower than the one recorded from the experiments and reported in Table 3. This discrepancies could be explained with the assumption of small deformations underpinning expression (3).

Fig. 5 and Fig. 6 show the overpressure required for sealing the microvalves. In particular, Fig. 5 shows the effect of the design parameter  $D_i$  for the membranes with diameter  $D = 800 \mu\text{m}$ , where Fig. 6 for the membranes

with a diameter  $D = 500 \mu\text{m}$ . Based on (3), the data for Fig. 5 have been fitted using:

$$\Delta P \propto (D^2 - D_i^2)^{-x} \quad (5)$$

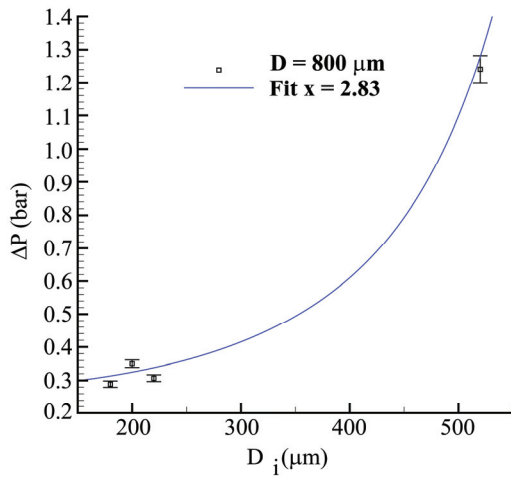


Figure 5: Actuating pressure for different ring dimensions, microvalves diameter  $D = 800 \mu\text{m}$ .

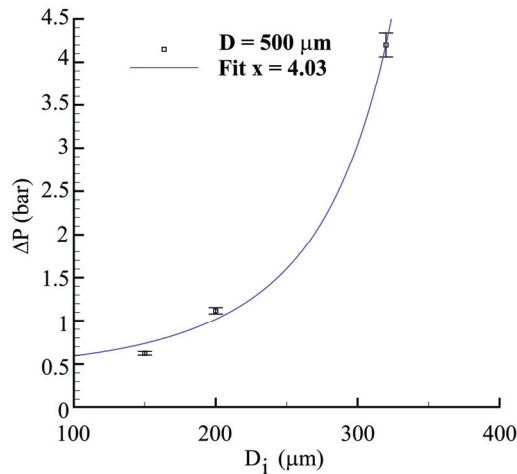


Figure 6: Actuating pressure for different ring dimensions, microvalves diameter  $D = 500 \mu\text{m}$ .

<b>D = 800 μm</b>	
$\Delta P_{V2}/\Delta P_{V1}$	1.21
$\Delta P_{V3}/\Delta P_{V1}$	4.30
<b>D = 500 μm</b>	
$\Delta P_{V5}/\Delta P_{V4}$	1.79
$\Delta P_{V6}/\Delta P_{V4}$	3.76

Table 3: Overpressure ratio for different ring values.

Table 4 shows the measured overpressure for microvalve V3 before and after it has been subjected to a continuous switching at 1Hz for 70 hours and at 2 Hz for 19

hours, corresponding to 250.000 and 137.000 actuating cycles respectively. It could be noted how the microvalve requires a slightly higher pressure to perfectly seal the carrier gas orifice after the heavy duty cycle.

Preliminary results for liquid microvalve, not reported in this work, also show perfect sealing, with an overpressure lower than 1 bar.

<b>P<sub>in</sub> (bar)</b>	<b>ΔP (bar) ± 3% ΔP</b>	
	<b>Before</b>	<b>After</b>
1.6	1.05	1.40
2.0	1.00	1.30
2.5	0.75	1.15

Table 4: Microvalve V3 overpressure before and after operating actuation cycles.

## CONCLUSIONS

In this work an SU-8 membrane for HSGC applications has been presented. Its advantages over more traditional membranes include the possibility to be integrated into a microfluidic circuit using standard MEMS technology at wafer level. The characterization of this microvalve showed the low overpressure required for sealing under different carrier gas pressures, and its ability to withstand heavy duty actuation cycles without any remarkable degradation of its mechanical properties.

## ACKNOWLEDGMENTS

This work was partially supported by Programma Operativo FESR 2007-2013 della Regione Emilia-Romagna – Attività I.1.1.

## REFERENCES

- [1] K.W. Oh and C.H. Ahn, “A review of microvalves,” *Journal of Micromechanics and Microengineering* 16, R13-R39, 2006.
- [2] K. Nachef, P. Guize, E. Dozier, B. Bourlon, “Microvalve and micro-fluidic devices using such,” *International Patent No.WO 2010/097740 A1*, 2010.
- [3] H.J. Ding, X.Y. Lee and W.Q. Chen, “Analytical solutions for a uniformly loaded circular plate with clamped edges,” *Journal of Zhejiang University Science*, 6A(10), 1163-1168, 2005.
- [4] E.I. Bromley, J.N. Randall, D.C. Flanders and R.W. Mountain, “A technique for the determination of stress in thin films,” *Journal of Vacuum Science & Technology B*, 1(4), 1364-1366, 1983.
- [5] A.T. Al-Halhouli, I. Kampen, T. Krah and Büttgenbach S., “Nanoindentation testing of SU-8 photoresist mechanical properties,” *Microelectronic Engineering*, 85, 942-944, 2008.